Target cascading in vehicle redesign: a class VI truck study

H.M. Kim, M. Kokkolaras, L.S. Louca, G.J. Delagrammatikas, N.F. Michelena, Z.S. Filipi, P.Y. Papalambros, J.L. Stein and D.N. Assanis

Department of Mechanical Engineering, University of Michigan, 2250 G.G. Brown Bldg., Ann Arbor, Michigan 48109–2125, U.S.A.

Abstract: The analytical target cascading process is applied to the redesign of a U.S. class VI truck. Necessary simulation and analysis models for predicting vehicle dynamics, powertrain, and suspension behaviour are developed. Vehicle design targets that include improved fuel economy, ride quality, driveability, and performance metrics are translated into system design specifications, and a consistent final design is obtained. Trade-offs between conflicting targets are identified. The study illustrates how the analytical target cascading process can reduce vehicle design cycle time while ensuring physical prototype matching, and how costly design iterations late in the development process can be avoided.

Keywords: design optimization, hierarchical modelling, target cascading, target setting, truck simulation, vehicle design.

Reference to this paper should be made as follows: Kim, H.M., Kokkolaras, M., Louca, L.S., Delagrammatikas, G.J., Michelena, N.F., Filipi, Z.S., Papalambros, P.Y., Stein, J.L. and Assanis, D.N. (2002) 'Target cascading in vehicle redesign: a class VI truck study', *Int. J. Vehicle Design*, Vol. 29, No. 3, pp. 199–225.

1 Introduction

The development of any complex product is strongly associated with matching specifications for each product attribute. Analytical target cascading [11,12] is a novel methodology for the design of large engineering systems at the early product development stages. First, the design problem is partitioned into a hierarchical set of subproblems associated with systems, subsystems, and components. Then, desired design specifications (or targets) are defined at the top level of the multilevel design formulation and 'cascaded down' to lower levels. Finally, design subproblems are formulated at each level to design components, subsystems, and systems that match cascaded targets and, hence, are consistent with overall product targets. The main benefits of target cascading are reduction in design-cycle time, avoidance of design iterations late in the development process, and increased likelihood that physical prototypes will be closer to production quality. Target cascading also facilitates

concurrency in system design: Once targets are identified for systems, subsystems, and components, the latter elements can be designed in detail independently, allowing their outsourcing to suppliers. Target cascading offers a robust framework for multilevel design and, using the results of Michelena *et al.* [17], has been demonstrated [11] to be convergent under standard convexity and smoothness assumptions, whereas other similar problem formulations exhibit convergence difficulties.

The scope of this study is to evaluate the analytical target cascading process on a U.S. class VI truck, which corresponds to a medium size, two-axle delivery vehicle. Vehicle dynamics, powertrain, and suspension responses are considered in the study. To apply the target cascading process, the vehicle design problem is decomposed using the bilevel hierarchy shown in Figure 1: the truck is represented at the top level, and engine, transmission, front suspension, and rear suspension systems are modelled at the bottom level. Two different sets of targets are specified for improving fuel economy, performance, ride quality, and driveability.

The article is organized as follows: The target cascading process is presented in the next section. The necessary analysis models for the vehicle and system levels are described in Section 3. Implementation issues of the truck redesign study are addressed in Section 4. Results are presented and discussed in Section 5. Finally, conclusions are drawn in Section 6.

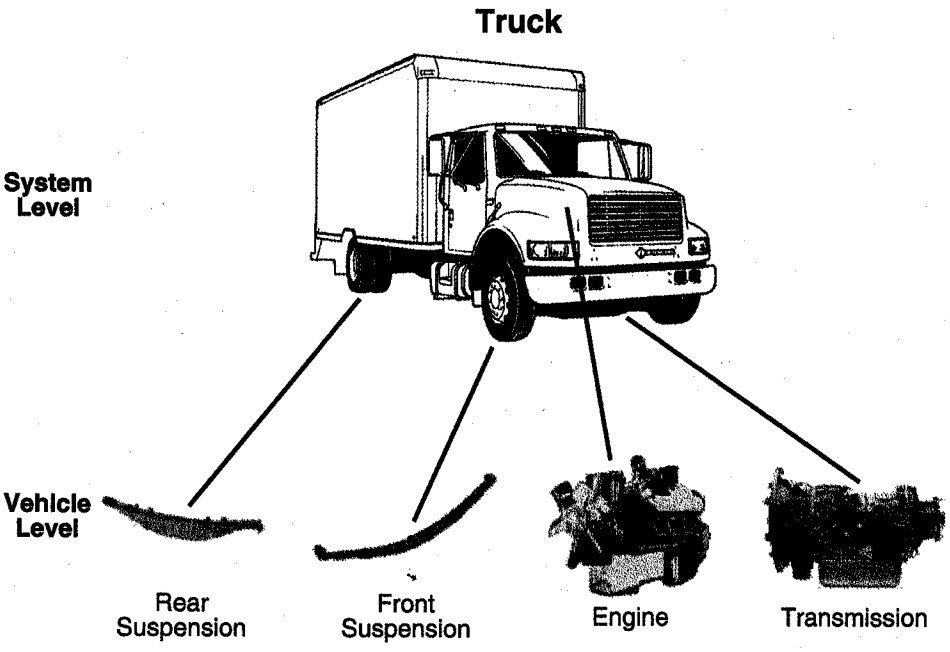

Figure 1 Model hierarchy for the U.S. class VI truck redesign study.

2 Target cascading formulation for optimal vehicle design

The mathematical formulation of the analytical target cascading process is presented in [12] for a general multilevel problem hierarchy. In this section the formulation is tailored for the bilevel hierarchy of the present study. Design problems are formulated for each element at the two levels, as described in the following subsections.

Before proceeding with individual problem formulations, some nomenclature and definitions are provided. A vector of targets $\mathbf{T}_v$ is introduced typically at the top level as the vehicle design requirements that need to be translated into design specifications for the systems. The vehicle and systems are referred to as the 'elements' of the hierarchy. Each element is associated with an analysis model used to estimate a vector of responses $\mathbf{R}$ that are assumed to be functions of local design variables $\mathbf{x}$ (associated exclusively with the element), linking design variables $\mathbf{y}$ (common with variables of other elements at the same level and having the same 'parent' element), and responses of lower-level elements. Response and linking variable values are passed up and down during the analytical target cascading process for coordination and design consistency reasons; superscripts $(\cdot)^L$ and $(\cdot)^U$ denote values passed up and down from the levels below and above, respectively. Figure 2 is provided to facilitate the following description of the design problems and the overall target cascading process.

2.1 Target cascading at the top (vehicle) level

At the vehicle level, responses $\mathbf{R}_v$ need to match desired vehicle design requirements $\mathbf{T}_v$ (cf. Figure 2). These responses are assumed to be functions of vehicle design variables $\mathbf{x}_v$ and system responses $\mathbf{R}_{S_i}$ for $i = 1, \ldots, n_s$ systems, i.e. $\mathbf{R}_v = \mathbf{r}_v(\mathbf{x}_v, \mathbf{R}_{S_1}, \ldots, \mathbf{R}_{S_{n_S}})$. To determine target values for system responses, determine vehicle design variables, and coordinate system linking variables a minimum

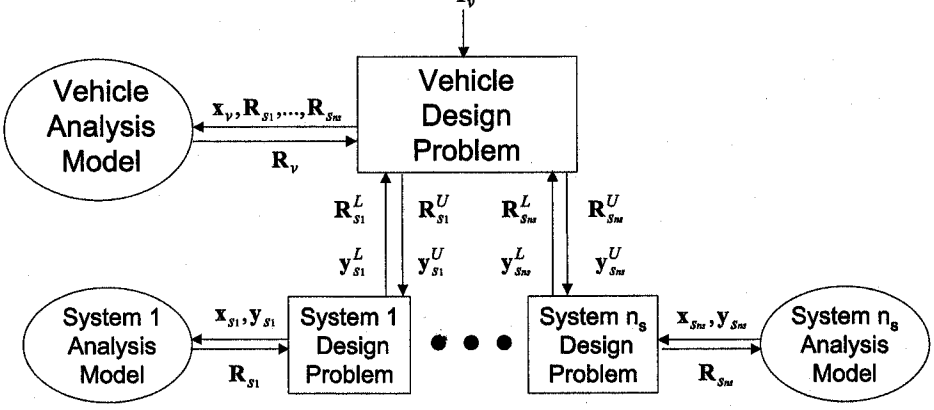

Figure 2 Schematic of the target cascading process for a bilevel hierarchy.

deviation optimization problem is formulated as follows:

$$\begin{aligned} &\min_{\bar{\mathbf{x}}_v} \quad ||\mathbf{R}_v - \mathbf{T}_v|| + \epsilon_V^R + \epsilon_v^y \\ &\text{subject to} \quad \sum_{i=1}^{n_s} ||\mathbf{R}_{s_i} - \mathbf{R}_{s_i}^L|| \leq \epsilon_v^R \\ &\sum_{i=1}^{n_s} ||\mathbf{y}_{s_i} - \mathbf{y}_{s_i}^L|| \leq \epsilon_v^y \\ &\mathbf{g}_v(\mathbf{R}_v, \mathbf{x}_v) \leq 0 \\ &\mathbf{h}_v(\mathbf{R}_v, \mathbf{x}_v) = 0 \end{aligned} \tag{1}$$

where

- $\bar{\mathbf{x}}_v = [\mathbf{x}_v, \mathbf{R}_{s_1}, \ldots, \mathbf{R}_{s_{n_s}}, \mathbf{y}_{s_1}, \ldots, \mathbf{y}_{s_{n_s}}, \epsilon_v^R, \epsilon_v^y]$ is the vector of optimization variables,
- $\mathbf{x}_v$ is the vector of design variables exclusively associated with the vehicle,
- $\mathbf{R}_v$ is the vector of vehicle responses,
- $\mathbf{R}_{s_i}$ is the vector of system responses for the i-th system,
- $\mathbf{y}_{s_i}$ is the vector of system linking design variables for the i-th system,
- ϵ_v^R is the tolerance variable for coordinating system responses,
- ϵ_v^y is the tolerance variable for coordinating system linking design variables,
- $\mathbf{T}_v$ is the vector of vehicle design target values,
- $\mathbf{R}_{s_i}^L$ is the vector of system response values passed up to the vehicle from the i-th system,
- $\mathbf{y}_{s_i}^L$ is the vector of system linking design variable values passed up to the vehicle from the i-th system,
- $\mathbf{g}_v$ and $\mathbf{h}_v$ are vector functions representing vehicle inequality and equality design constraints, respectively, and
- $||\cdot||$ is some norm; typically, some weighted norm is used for the metrics involving the targets $\mathbf{T}_v$ in order to enable trade-off evaluation studies, while the l_2-norm is used in all other cases.

2.2 Target cascading at the bottom (system) level

Once optimal values for the system responses $\mathbf{R}_{s_i}$ and system linking design variables $\mathbf{y}_{s_i}, i = 1, \ldots, n_s$, are determined by solving optimization problem (1) at the vehicle level, they are cascaded down to the system level as target values $\mathbf{R}_{s_i}^U$ and $\mathbf{y}_{s_i}^U$, respectively (cf. Figure 2). At the system level, n_s individual minimum deviation optimization problems are formulated to determine system design variables and system linking variables. Given that in this particular study the system level corresponds to the bottom level of the problem hierarchy, system responses are assumed to be functions of system local design variables and system linking design variables, i.e. $\mathbf{R}_{s_i} = \mathbf{r}_{s_i}(\mathbf{x}_{s_i}, \mathbf{y}_{s_i})$. The optimization problem for each system s_i,

$i = 1, \ldots, n_s$, is as follows:

$$\begin{aligned} &\min_{\bar{\mathbf{x}}_{s_i}} ||\mathbf{R}_{s_i} - \mathbf{R}_{s_i}^U|| + ||\mathbf{y}_{s_i} - \mathbf{y}_{s_i}^U|| \\ &\text{subject to } \mathbf{g}_{s_i}(\mathbf{R}_{s_i}, \mathbf{x}_{s_i}, \mathbf{y}_{s_i}) \leq 0 \\ &\qquad\qquad \mathbf{h}_{s_i}(\mathbf{R}_{s_i}, \mathbf{x}_{s_i}, \mathbf{y}_{s_i}) = 0 \end{aligned} \tag{2}$$

where

- $\bar{\mathbf{x}}_{s_i} = [\mathbf{x}_{s_i}, \mathbf{y}_{s_i}]$ is the vector of optimization variables,
- $\mathbf{x}_{s_i}$ is the vector of system design variables exclusively associated with the i-th system,
- $\mathbf{R}_{s_i}^U$ is the vector of system response target values for the i-th system passed down from the vehicle level,
- $\mathbf{y}_{s_i}^U$ is the vector of system linking design variable values for the i-th system passed down from the vehicle level, and
- $\mathbf{g}_{s_i}$ and $\mathbf{h}_{s_i}$ are vector functions representing inequality and equality design constraints for the i-th system, respectively.

Once optimal values for the system responses $\mathbf{R}_{s_i}$ and system linking design variables $\mathbf{y}_{s_i}, i = 1, \ldots, n_s$, are determined by solving optimization problem(s) (2) at the system level, they are passed up to the vehicle level as parameters $\mathbf{R}_{s_i}^L$ and $\mathbf{y}_{s_i}^L$, respectively.

3 Description of models

Appropriate vehicle and system analysis models that take design variables as input and compute responses as output are necessary to implement the target cascading process. At the vehicle level, the integrated system was modelled using the 20SIM [1] modelling environment to predict responses corresponding to truck targets. This model is described in Section 3.1. The vehicle model contains submodels of the engine, drivetrain, and vehicle dynamics, which are described in Subsections 3.1.1, 3.1.2, and 3.1.3, respectively. At the system level, higher fidelity models were used to predict responses of the engine, transmission, and suspensions. These models are described in Subsections 3.2.1, 3.2.2, and 3.2.3, respectively.

3.1 Vehicle-level model

The schematic of the vehicle is depicted in Figure 3. A diesel engine delivers power to a torque converter (TC), whose output shaft is coupled to a transmission (T), propeller shaft (PS), differential (D) and two driveshafts (DS), which couple the differential with the rear driven wheels. The vehicle has solid front and rear axles with leaf spring suspensions. This configuration represents a 4×2 delivery truck of the International Truck and Engine Corporation 4700

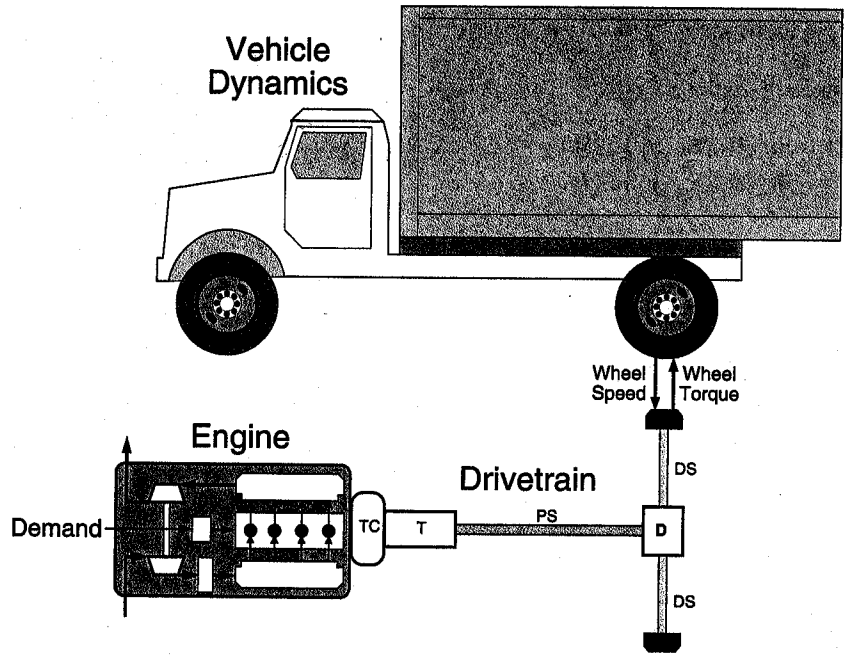

Figure 3 Schematic of the integrated vehicle system.

series with a 4-speed automatic transmission; however, the same configuration with minor modifications can be used for modelling other two-axle vehicles.

The basis for the vehicle-level model is the vehicle-engine-simulation (VESIM) developed in SIMULINK [22] at the University of Michigan and validated against measurements from proving grounds for a production class VI truck [3]. The simulation has been updated to improve its computational efficiency through an approach that includes application of model reduction methodologies to individual system modules and implementation in a software environment capable of producing compact stand-alone code. Thus, the vehicle model [16] was generated using the 20SIM [1] modelling environment, which supports hierarchical structuring and allows physical modelling by means of bond graphs [10,21], block diagrams, or direct equation formulations. A hierarchical approach was necessary given the complexity of the vehicle.

The vehicle model was decomposed into submodels such as engine, drivetrain, and vehicle dynamics that are excited by the environment (i.e. driver and road) as shown in Figure 4. The representation in Figure 4 includes both bond and signal connections between submodels. A bond connection denotes the power flow and causality between two components, e.g. engine and drivetrain. One source of excitation is the driver who controls the vehicle velocity through the gas and brake pedals in order to maintain the velocity dictated by the driving cycle. Another source of excitation is the road profile. Road excitation is applied to both front and rear tyres as a function of their longitudinal position. The driver can also control the vehicle heading through the steering wheel; however, steering input is neglected since the design study focuses on ride and performance characteristics. The vehicle model

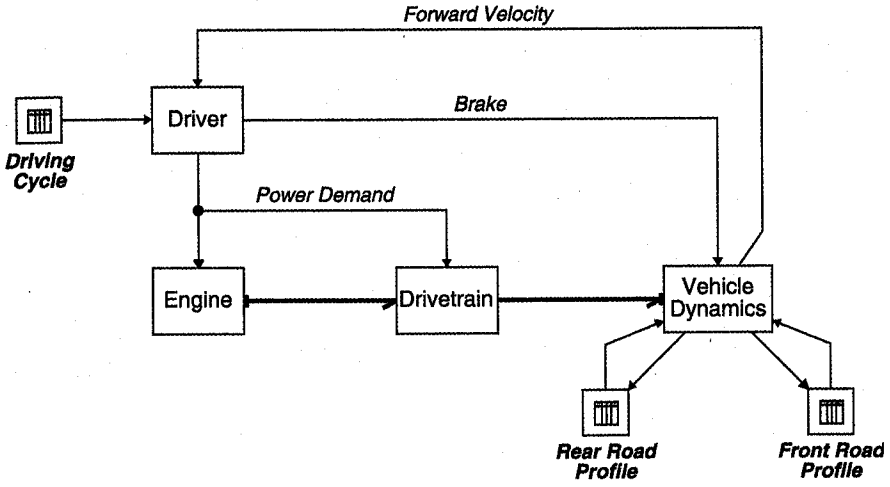

Figure 4 Vehicle model representation.

is constrained to move only on the pitch plane, and has three degrees of freedom (longitudinal, heave, and pitch).

Following validation of vehicle responses as measured during a performance manoeuvre, models were reduced to improve overall computational efficiency. The reduced engine model was derived from the high fidelity, thermodynamic engine system model described in [3,4]. Reduction requires replacing the thermodynamic engine model by a look-up table that provides brake torque as a function of engine speed and mass of fuel injected per cylinder per cycle. The process of generating look-up tables for different engine designs is described in Section 3.1.1. The complete fuel control logic was kept in the look-up table based model to retain critical transient engine response features, as shown in Figure 5. In addition, a carefully calibrated time delay was built-in to represent the effect of turbo-lag on transient response to rapid increases of torque demand. The complexity of the drivetrain and vehicle dynamics submodels was reduced using model reduction techniques [14,15]. Elements that do not contribute to the outputs of interest were eliminated, while retaining design variables with physical meaning. Starting with the maximum possible complexity, the energy-based model order reduction algorithm (MORA) was applied to models using the baseline set of parameters and a rich input to excite all system dynamics [16].

In the next subsections, engine, drivetrain, and vehicle dynamics submodels within the vehicle model are briefly described. A more detailed description of the submodels can be found in [16,3].

3.1.1 Engine submodel

The engine submodel, shown in Figure 5, includes the inertial effects of all rotating parts and energy losses due to friction, which are lumped into single port elements **I** and **R**, respectively. The effort source **Se** represents the engine brake torque given by a steady state look-up table as a function of engine speed and fuelling rate. These

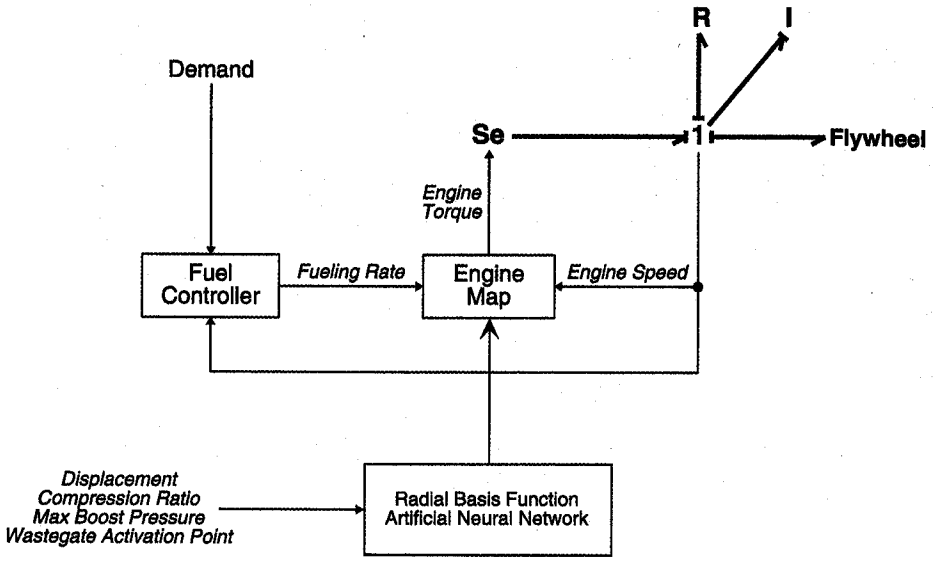

Figure 5 Engine submodel within the vehicle model.

bond graph elements are connected by means of the junction structure element '**1**', which denotes engine speed. Engine power is controlled by a fuel injection controller, which provides the signal for the mass of fuel injected per cycle based on driver demand and engine speed. Special functions include corrections for insufficient boost pressure, governing function for prevention of overspeeding, and a carefully calibrated time delay representing the effect of turbo-lag on transient response. More details of the engine submodel are provided in [3,13].

Typically, engine lookup tables are obtained from measurements of actual engines. However, one would have to treat the entire engine map as a design variable to study the behaviour of a vehicle for a range of engine designs. Representative engine parameters can be treated as design variables to avoid increasing the size of the design problem. This approach requires an extensive amount of expensive computations, unless a surrogate model is used to generate the engine map for combinations of engine design variables. Thus, a series of engine maps were generated by means of a high fidelity engine model (described in Section 3.2.1) and used to train an artificial neural network (ANN). The training process is described in more detail in the remainder of this section.

The efficient function `newgrnn` of the MATLAB Neural Network Toolkit [7] was used to design a generalized regression neural network using radial basis functions. Such networks are often used for function approximation and are preferred to feed-forward neural networks because training time is much shorter and there are no tuning parameters other than the spread of the radial basis functions. Moreover, training algorithm and network architecture (i.e. number of layers and neurons) do not have to be defined by the user. The Matlab Neural Network Toolkit also provides for normalization of the data used for training and simulating the network.

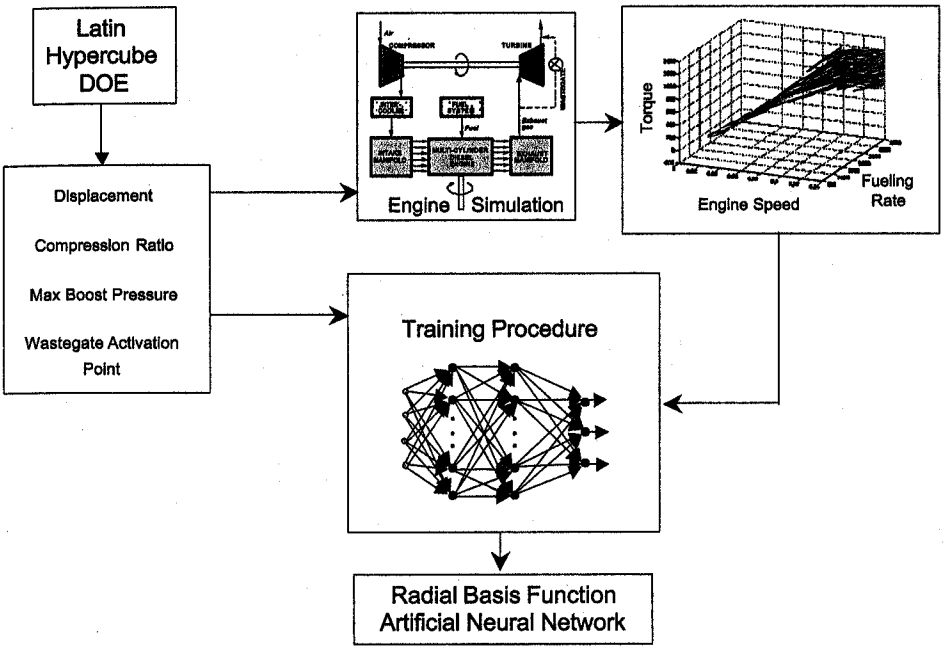

Figure 6 Artificial neural network training procedure.

Four engine design parameters were chosen as input to the neural network: displacement, compression ratio, maximum boost pressure (controlled by a wastegate), and engine speed corresponding to the wastegate activation point. A design of experiments (DOE) based on a Latin hypercube was performed to produce data to train the network. After setting lower and upper bounds for the four input parameters, 500 hypercubes of dimension 100 were computed (i.e. each of the four parameters was sampled at 100 positions). Euclidean distances between all points of each hypercube were then computed. Finally, the hypercube with the greatest minimum distance between its points was chosen as the one with the most dispersed points. Engine maps were then generated for the 100 combinations of the four input parameters using the high fidelity engine model described in Section 3.2.1. The artificial neural network was trained using these input-output relations. The complete process is illustrated in Figure 6. A cross-validation error analysis showed that the mean average relative error and the associated standard deviation were approximately 8% and 5%, respectively. These values are considered satisfactory for the desired fidelity of the engine submodel at the vehicle level.

3.1.2 Drivetrain submodel

The drivetrain submodel consists of the torque converter, transmission, propshafts, differential, drive shafts, and shift logic, and connects engine and vehicle dynamics through the pump and shaft ports, respectively, as illustrated in Figure 7. The torque converter input shaft, on one end, and the drive shaft, on the other end, are the connecting points for the engine and the vehicle dynamics submodels, respectively.

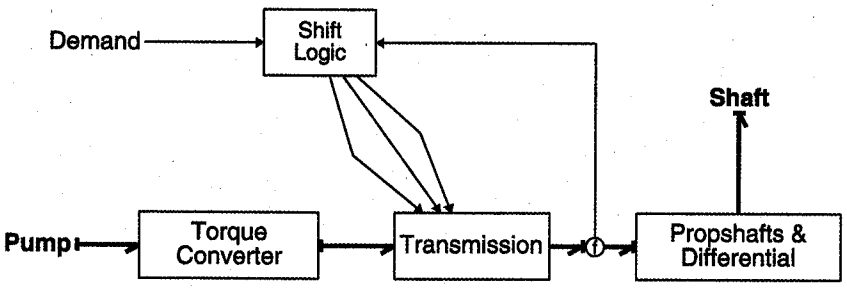

Figure 7 Drivetrain submodel within the vehicle model.

As dictated by causality, the inputs are the engine and wheel rotational speeds, and the outputs are the torque to the wheels and load torque on the engine. An additional input is the driver demand signal, which is used by the shift logic.

The torque converter is a fluid clutch by which the engine is coupled to the transmission. The typical three-element torque converter consists of a pump, stator, and turbine. The pump is connected rigidly to the engine flywheel, and the turbine to the transmission input shaft. The stator is connected to the torque converter housing via a one-way clutch. The presence and arrangement of the stator cause the torque converter to act as a torque multiplication device when operating at low speed ratios, and as an approximately direct drive fluid coupling at higher speed ratios. The fluid coupling has characteristics of a gyrator (a bond graph junction structure element) since the pump and turbine torques are determined by the turbine and pump speeds. The gyrator modulus is calculated from quasi-static experimental data using an empirical capacity factor and torque multiplication quantities. The model also includes turbine inertia.

The central element of the transmission is a non-power conserving transformer that includes gear efficiency and allows different transmission gears. Speed reduction in each gear is assumed ideal, while torque multiplication is reduced by the appropriate gear efficiency factor. The transmission model consists of a series spring-inertia-spring arrangement and the non-power conserving transformer (gear ratio) in between. Viscous dampers that account for structural damping are in parallel with the springs. These ideal elements represent the equivalent inertia and compliance of the gears and shafts. Fluid churning and charging pump losses were also modelled. The transmission model was reduced using the activity metric in the model order reduction algorithm, which identifies and eliminates compliant elements that are not important with respect to outputs of interest. As a consequence, input and output transmission speeds are algebraically related.

The driveline includes two propshafts joined by a universal joint. The propshafts were modelled as an inertia-spring-inertia-spring-inertia series arrangement with small viscous damping in parallel with the springs. Following the propshafts is the differential, which includes an input compliance, axle inertia, and output compliance. The model includes the cooler fluid churning losses for the differential/axle. The differential was modelled as a non-power conserving transformer with ideal speed reduction but non-ideal torque multiplication based on a given gear efficiency. After applying the activity metric to the driveline model, the compliances of the propshafts and the input differential were eliminated. The final model includes only output differential compliance and rotational inertias.

The last component of the drivetrain is the shift logic module, which given the transmission output shaft speed and the driver demand determines the gear the transmission should be in. It uses a gearshift map, provided by the International Engine and Truck Corporation, that determines the current gear number, and whether or not an upshift or downshift event is to be initiated. During gearshift speed reduction and torque multiplication, ratios vary from initial to final values according to blending functions, which model torque and speed ratio variations as clutches and bands engage and disengage. The shift logic is described by a set of logical statements.

3.1.3 Vehicle dynamics submodel

The vehicle dynamics submodel includes wheels, tyres, axles, suspensions, and the frame of the vehicle. The vehicle was modelled as a collection of rigid bodies that are allowed to move on the 2-dimensional plane subject to forces, moments, and rigid constraints (cf. Figure 8). Forces and moments act at specific points of two bodies, e.g. the rear suspension acts between point SR of the axle and point R of the frame. In addition, two bodies can be restrained to move only in a specific direction or trajectory by a rigid constraint, e.g. the front axle is constrained to move on the y^f-axis of the frame.

The vehicle dynamics submodel is connected to the drivetrain submodel at the rear driven wheels. Researchers have developed models of a half car using the bond graph approach; e.g. Pacejka and Tol [20] developed a simplified linear model by assuming small pitch angles. In this work we are interested in a wider range of pitch motion that makes the suggested bond graph representation more complex and difficult to manipulate. Therefore, a hierarchical modelling approach was used, where

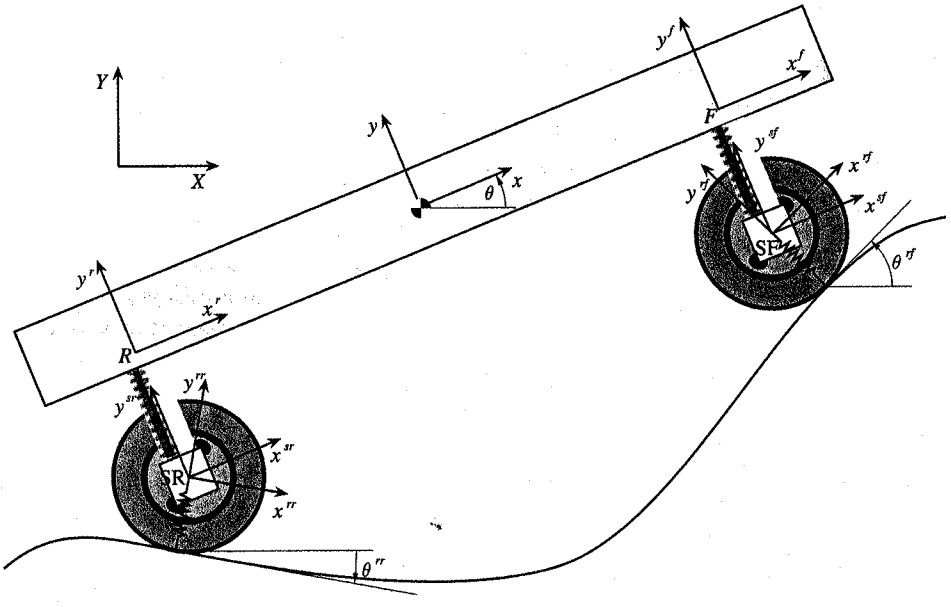

Figure 8 Half car model schematic.

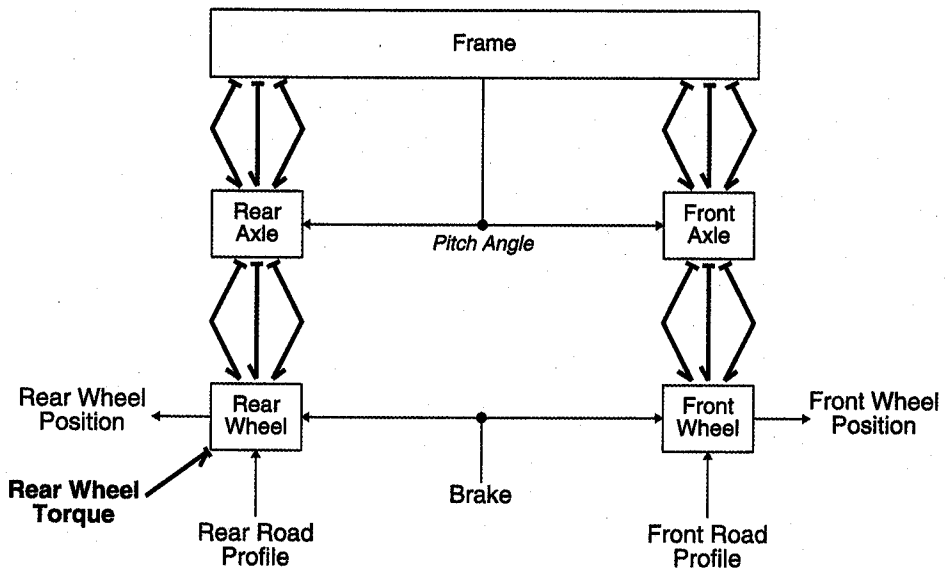

Figure 9 Vehicle dynamics submodel within the vehicle model.

the vehicle is decomposed into the frame, front axle, front wheel, rear axle, and rear wheel, as shown in Figure 9. The frame was modelled as a rigid body that is allowed to move horizontally and vertically, and to pitch. Three inertial elements represent the dynamics in the three degrees of freedom. The kinematics are described in a body fixed frame and represented by the nonlinear Euler equations. The gravity force is applied at the centre of gravity (CG) location after transforming the CG velocity in the inertial (X, Y) frame. This transformation is a standard coordinate rotation around the out-of-plane axis. The frame also includes two points for connecting the front and rear axles. Each point is located at a constant position (x_F, y_F) and (x_R, y_R) relative to the CG. Finally, the aerodynamic drag was modelled by energy losses that are quadratic in the forward vehicle velocity. Each axle was modelled as a rigid body with its kinematics described in the body fixed frame. The axle is constrained by a rigid constraint to move on an axis that has its origin at the attachment point F or R and is perpendicular to the horizontal axis of the frame (x^f, y^f) or (x^r, y^r), respectively. The axle is also constrained by the suspension that was modelled as a linear spring and damper connected in parallel. Finally, gravity force is applied to the axle through transformation of velocities from the local to the global frame.

The tyre model includes the wheel dynamics and the interaction of the tyre with the road. The wheel mass is lumped into the axle to avoid more kinematic constraints and computational inefficiencies. The model includes the wheel moment of inertia and bearing viscous losses at the wheel hub. The drive torque from the drivetrain is applied to the hub to accelerate the wheel. A simple brake model with viscous and Coulomb friction generates the required torque for decelerating and stopping the vehicle. Tyre rolling resistance was added to the model as an additional source of energy losses. Tyre forces in the vertical direction were modelled as a linear spring and damper connected in parallel. The model can also predict wheel lift off. The

longitudinal traction force is calculated using the Pacejka model taken from the work of Pacejka and Bakker [19]. First, the axle velocity at point *SF* (*SR*) is converted in a frame that is aligned with the road at the contact point. This coordinate transformation gives the forward velocities of the contact point *SF* (*SR*) in the (x^{tf}, y^{rf}) $((x^{tf}, y^{rr}))$ that is used to calculate the wheel slip. Finally, the traction force is calculated as a nonlinear function of wheel slip and normal load. This function is given by Pacejka's model and its constants are estimated from measured data of the actual tyre.

The vehicle dynamics submodel was also reduced using the activity metric in MORA. Tyre damping and vertical inertial effects of the front and rear unsprung masses were found to be unimportant for the manoeuvres of interest (acceleration and braking). The elimination of these elements improves the computational efficiency by removing high frequency dynamics.

3.2 System-level models

The four elements at the system level include the engine, transmission, front suspension, and rear suspension. Within the target cascading methodology, these models are typically of higher fidelity compared to their counterparts within the vehicle-level model.

3.2.1 Engine model

The turbocharged diesel engine simulation (TDES) used as the high fidelity engine model is a modified version of the FORTRAN code first developed by Assanis and Heywood [4]. TDES is a zero-dimensional, quasi-static, feed-forward engine simulation that predicts engine outputs at a single operating point (i.e. engine speed and fuelling rate combination). The diesel four-stroke cycle is treated as a sequence of continuous processes: intake, compression, combustion (including expansion), and exhaust. Quasi-steady, adiabatic, one-dimensional flow equations are used to predict mass flows past the intake and exhaust valves. Combustion was modelled as a uniformly distributed heat release process using Watson's correlation [25]. Convective heat transfer in the combustion chamber was modelled using a Nusselt number correlation, based on turbulent flow in pipes, and the characteristic velocity concept [4], for evaluating the turbulent Reynolds number in the cylinder. The characteristic velocity and length scales required by these correlations are obtained from an 'energy cascade' zero-dimensional turbulence model [23]. Radiative heat transfer is added during combustion [8]. The combustion chamber surface temperatures of the piston, cylinder head, and liner can be either specified or calculated from a specification of the wall structure. A friction sub-model based on the correlation of Millington and Hartles [18] predicts engine friction losses and converts indicated to brake quantities. The interaction between the master cylinder model and the other components is accounted for in the manifolds modelled as separate control volumes. Instantaneous mixing of all mass flows with the gases already in their respective manifolds is assumed. To complete the system, a compressor is connected to the inlet side of the intake manifold and a turbine is connected to the outlet side of the exhaust manifold. The turbocharger model is based on a 2-dimensional interpolation of digitized compressor and turbine performance maps. Scaling of turbomachinery, necessary when engine displacement

is changed, is performed using fundamental equations for turbocharger design [24]. Finally, a predictive wastegate model, which consists of a spring-loaded diaphragm in the exhaust manifold, is included in the simulation [2].

In its original form, TDES can only predict engine outputs for a single operating point, given a specific fuelling rate and speed combination. An automated procedure was developed and implemented in a FORTRAN code to produce an entire engine map. First, the maximum torque curve for every engine design was calculated using a modified Newton-Raphson technique [6]. The fuelling rate associated with the maximum load on the maximum torque curve defined the upper bound of the fuel axis; the lower bound was then set at 25% of this value. After the speed range and the number of increments on each axis were specified, each speed and fuel combination was input to TDES. The output torques were then calculated and indexed on their respective map positions. The variables of the engine design problem are displacement, compression ratio, maximum boost pressure (controlled by a wastegate), wastegate activation point, instantaneous inlet manifold pressure, and injection timing. The computed response is the engine map, i.e. torque as a function of engine speed and fuelling rate.

3.2.2 Transmission model

A model was employed at the system level to design a transmission that matches the gear ratios determined using the simplified transmission submodel at the vehicle level. The transmission is shown in Figure 10 and consists of two planetary gears (input and reaction). The input and reactions planet carriers are mechanically connected with the reaction and input ring gears, respectively. Engagement or disengagement of the three clutches results in four forward and one reverse gear

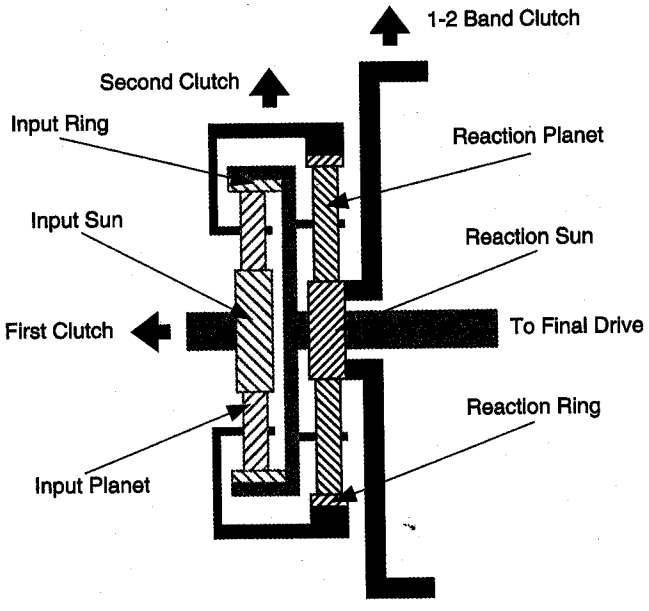

Figure 10 Transmission planetary systems.

ratios between the input and output shafts of the transmission. These gear ratios are determined by the teeth number of the ring and sun gears. Since there are two planetary systems, the gear ratios depend on four gear teeth numbers: the input sun (N_s^I), input ring (N_r^I), reaction sun (N_s^R) and reaction ring (N_r^R). The four gear ratios are given by the following relations:

$$G_1 = \frac{1 - R_r^I R_r^R}{R_s^I R_r^R}, \quad G_2 = \frac{1}{R_r^R}, \quad G_3 = \frac{1 - R_s^I}{R_r^I}, \quad G_4 = R_r^I \tag{3}$$

where

$$R_s^I = \frac{N_s^I}{N_s^I + N_r^I}, \quad R_r^I = \frac{N_r^I}{N_s^I + N_r^I}, \quad R_s^R = \frac{N_s^R}{N_s^R + N_r^R}, \quad R_r^R = \frac{N_r^R}{N_s^R + N_r^R} \tag{4}$$

The design variables of the transmission design problem are the number of teeth for the input sun, reaction sun, input ring, and reaction ring. The computed responses are the four gear ratios.

3.2.3 Suspension model

A model was used to design a suspension that matches the compliance and damping determined at the vehicle level. The suspension has a leaf spring configuration where n steel leaves are layered on top of each other (cf. Figure 11) providing stiffness characteristics through bending and damping characteristics through friction losses between the leaf contact surfaces. All leaves have same thickness t and width w. The top leaf has length L_1 and curvature radius R_1; subsequent leaves have linearly decreased lengths and curvature radii that are incrementally increased by the leaf thickness. Given these properties and using standard solid mechanics theory, the total stiffness is calculated as:

$$K = \frac{32\ E\ I\ SF}{L_t^3} \tag{5}$$

where

$$I = n\left(\frac{wt^3}{12} + 0.01354t^4\right) \tag{6}$$

and

$$L_t = R_1\sqrt{2 - 2\cos\left(\frac{2L_1}{R_1}\right)} \tag{7}$$

In the above equations, E is the Young modulus of the leaf material and SF is a stiffening factor. The dissipated energy for a step displacement input is used for the damping calculations. This is necessary given that the vehicle-level submodel uses linear viscous damping, whereas the leaf spring model has dry friction damping. Therefore, energy is used as a universal metric to design both linear viscous and dry

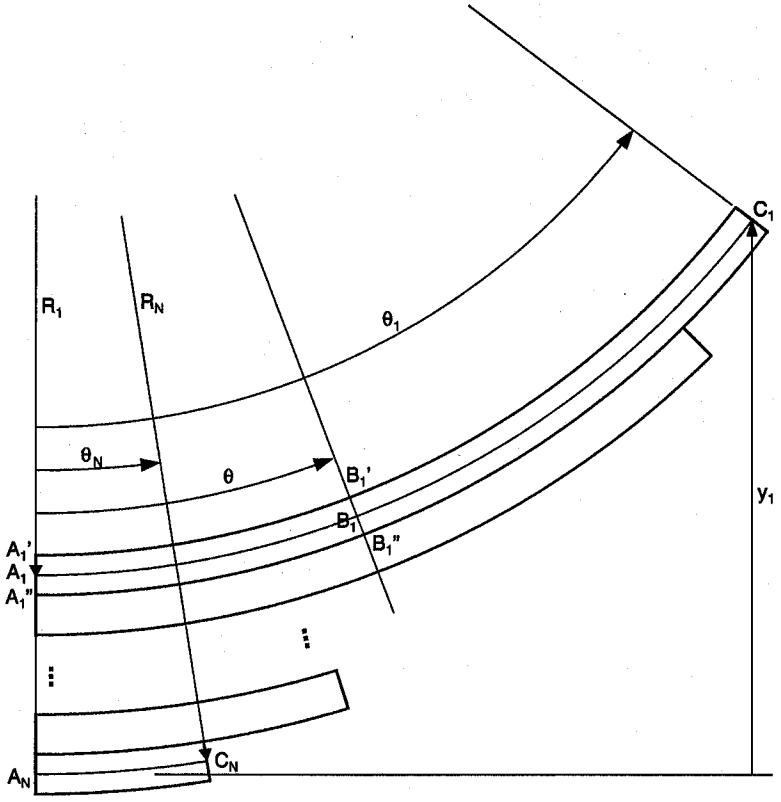

Figure 11 Leaf spring schematic.

friction damping. For the linear viscous damping the energy E_D is given by

$$E_D = \frac{A^2 B}{2} \tag{8}$$

where A is the amplitude of the input and B is the viscous damping parameter.

The equation for the total energy E_T of the leaf spring suspension system is then given by

$$E_T = K\mu t A^2 \frac{\partial R_1}{\partial y_1} \sum_{i=1}^{n-1} \left(\frac{1}{R_i} + \frac{1}{R_{i+1}}\right) \frac{1}{\theta_{i+1}} (\cos(\theta_{i+1}) + \theta_{i+1} \sin(\theta_{i+1}) - 1) \tag{9}$$

where

$$\frac{\partial R_1}{\partial y_1} = 2 \sin\left(\frac{\theta_1}{2}\right) \left(\sin\left(\frac{\theta_1}{2}\right) - \frac{\theta_1}{2} \cos\left(\frac{\theta_1}{2}\right)\right) \tag{10}$$

and μ is the Coulomb friction coefficient between the leaves.

The design variables of the suspension design problem are the number, thickness, and width of leaves, and the curvature radius of the top leaf. The computed responses are the compliance (i.e. the reciprocal of the stiffness) and damping of the suspension system.

4 Implementation issues

The redesign study of the U.S. class VI truck illustrates the target cascading process when applied to the bilevel hierarchy shown in Figure 1. Following the formulation in Sections 2.1 and 2.2 and the illustration in Figure 2, the target cascading hierarchy consists of one vehicle design problem at the top level and four system design problems at the bottom level. The coordination and information flow is illustrated in Figure 12. Targets, local design variables, and responses are shown in octagons, optimizers (solving the problems in Equations (1) and (2)) are shown in rectangles, and analysis models are shown in ovals.

The vehicle-level problem is solved first: vehicle targets $\mathbf{T}_v$ are set to be matched by vehicle responses $\mathbf{R}_v$; these include fuel economy, ride quality, driveability, and performance. Fuel economy is measured in miles per gallon and computed by dividing the travelled distance by the consumed fuel after completion of the driving cycle. Ride quality and driveability are associated with average vertical and horizontal accelerations of the vehicle's centre of gravity, respectively, and obtained by computing the squared root of the integrals of the squared accelerations over the driving cycle time period. Performance is characterized by the vehicle's 0–60 mph

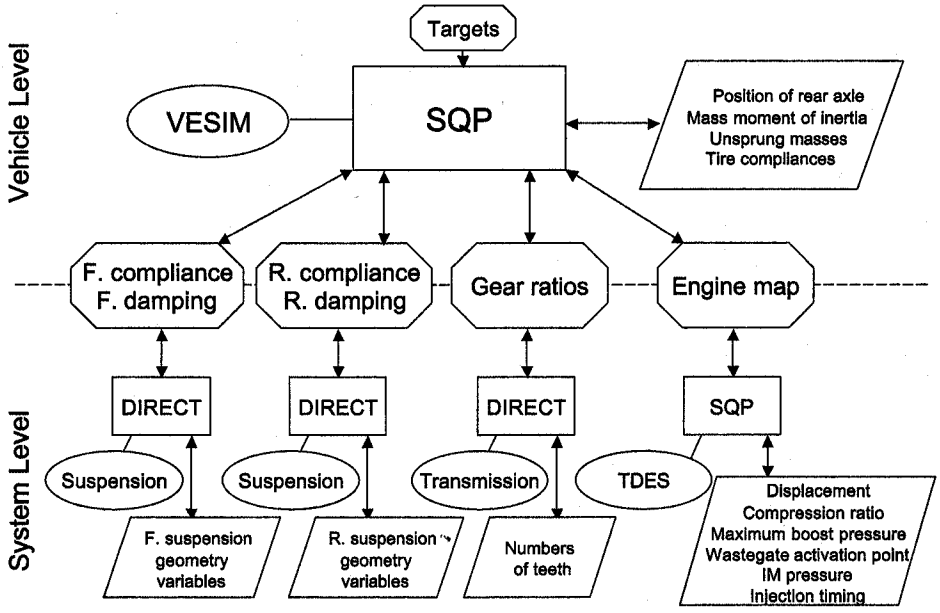

Figure 12 Coordination and information flow of the analytical target cascading process.

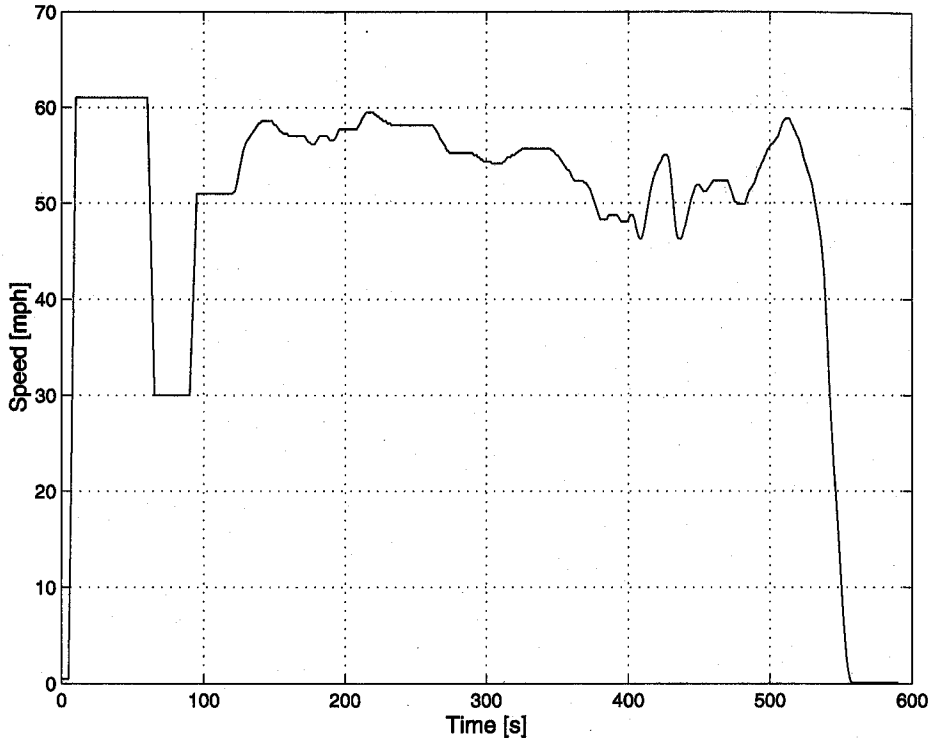

Figure 13 Driving cycle.

and 30–50 mph times. The driving cycle necessary to evaluate the above attributes is shown in Figure 13. This cycle was designed such that performance of the truck is evaluated at the beginning of the simulation, while fuel economy is determined during the second part of the simulation. The latter is based on the last 400 s of the U.S. federal highway driving cycle. A horizontal and smooth road profile was assumed throughout the driving cycle.

The optimization variables vector $\bar{\mathbf{x}}_v$ for the design problem at the top level consist of local design variables $\mathbf{x}_v$ and system responses $\mathbf{R}_{s_i}$, $i = 1, 2, 3, 4$. Local design variables $\mathbf{x}_v$ include vehicle mass moment of inertia, positioning of rear axle relative to the centre of gravity, front axle unsprung mass, front tyre compliance, rear axle unsprung mass, and rear tyre compliance. Assuming that $[s_1, s_2, s_3, s_4]$ corresponds to [*fsusp*, *rsusp*, *tra*, *eng*], system responses include front suspension responses $\mathbf{R}_{fsusp}$, rear suspension responses $\mathbf{R}_{rsusp}$, transmission responses $\mathbf{R}_{tra}$, and engine responses $\mathbf{R}_{eng}$. Suspension, transmission, and engine responses consist of compliance and damping, gear ratios, and the engine torque map, respectively. Note that the engine map was not treated as an optimization variable directly; instead, the four input parameters of the artificial neural network described in Section 3.1.1 were treated as optimization variables and the network output (i.e. the engine map) was used within VESIM. Lower and upper bounds for the optimization variables were set at $\pm 15 - 30\%$ of the baseline values, depending on the variable. The sequential

quadratic programming (SQP) algorithm of the MATLAB Optimization Toolbox [5] was used as optimizer.

Once response values $\mathbf{R}_{s_i}$, $i = 1, 2, 3, 4$, have been determined by solving the vehicle-level problem, they are cascaded down to the system level as targets $\mathbf{R}^U_{s_i}$, $i = 1, 2, 3, 4$, where four problems are solved independently to match them. The local design variables $\mathbf{x}_{eng}$, $\mathbf{x}_{tra}$, and $\mathbf{x}_{fsusp}$ and $\mathbf{x}_{rsusp}$ for the engine, transmission, and suspension systems were described in the last paragraphs of Sections 3.2.1, 3.2.2, and 3.2.3, respectively. Note that there are no system linking variables $\mathbf{y}_{s_i}$, i.e. none of the four system problems share any optimization variables. Due to the presence of integer variables, the derivative free optimization algorithm DIRECT [9] was used for the two suspension and the transmission problems, while the SQP algorithm was used for the engine map matching problem.

Solving the system-level problems completes one iteration of the target cascading process. The updated system response values $\mathbf{R}_{s_i}$, $i = 1, 2, 3, 4$, are passed up to the vehicle level as constraint targets $\mathbf{R}^L_{s_i}$, $i = 1, 2, 3, 4$, where the vehicle-level problem is solved again. If the matching of responses is not satisfactory the whole process is repeated in an iterative manner until convergence within some tolerance is achieved.

Two sets of targets were used for the redesign study, referred to as A and B. For target set A an improvement of at least 20% over baseline attribute values, except for the vertical acceleration, was attempted. For target set B specific target values were not defined; instead it was attempted to improve all attributes as much as possible. The target values of both sets are summarized in Tables 1 and 2. Note that the overall objective of the redesign study is to increase fuel economy and decrease the rest of the attributes.

Table 1 Baseline, target, and final values for target set A.

Response	Baseline value	Target value	Final value	Improvement
Fuel economy [mpg]	12.27	15.5	14.61	20.05%
Average horizontal acceleration [m/s^2]	44.57	35	45.27	−1.57%
Average vertical acceleration [m/s^2]	1.53	1.5	1.29	15.69%
0–60 time [s]	35.66	29.0	34.12	4.32%
30–50 time [s]	16.12	13.0	15.18	5.83%

Table 2 Baseline, target, and final values for target set B.

Response	Baseline value	Target value	Final value	Improvement
Fuel economy [mpg]	12.27	∞	13.65	12.16%
Average horizontal acceleration [m/s^2]	44.57	0	48.62	−9.09%
Average vertical acceleration [m/s^2]	1.53	0	1.15	24.84%
0–60 time [s]	35.66	0	27.92	21.70%
30–50 time [s]	16.12	0	13.06	18.98%

5 Results and discussion

The target cascading process converged after two iterations for both target sets. This is not surprising considering that the baseline design corresponds to an existing truck. Table 1 presents the obtained responses for target set A. It can be seen that a 20% improvement for all attributes cannot be achieved. Only the target for ride quality (measured in terms of average vertical acceleration) is met; this is not an extraordinary achievement considering that the baseline design was almost meeting this target. Nevertheless, a substantial improvement is achieved for fuel economy, while performance (related to 0–60 and 30–50 mph times) is improved moderately. It is also observed that driveability (associated with average horizontal acceleration) is deteriorated; an obvious trade-off exists between improving performance and driveability. This is expected since efforts to improve the truck performance are conflicting with efforts to improve its driveability. However, both targets are included in the problem formulation because it is desired to keep horizontal acceleration as low as possible even if it is known *a priori* that neither the target value nor an improvement can be reached.

To investigate whether or not some of the metrics under consideration can be improved further and to establish more potential trade-off relations, the target cascading process was repeated without specific numerical values as targets (target set B). The optimization process attempts in this case to improve the attributes of interest as much as possible. The obtained responses are summarized in Table 2. Target achievements for target sets A and B can be visualized in the charts of Figures 14 and 15, respectively. For target set A, baseline and final values are normalized with respect to

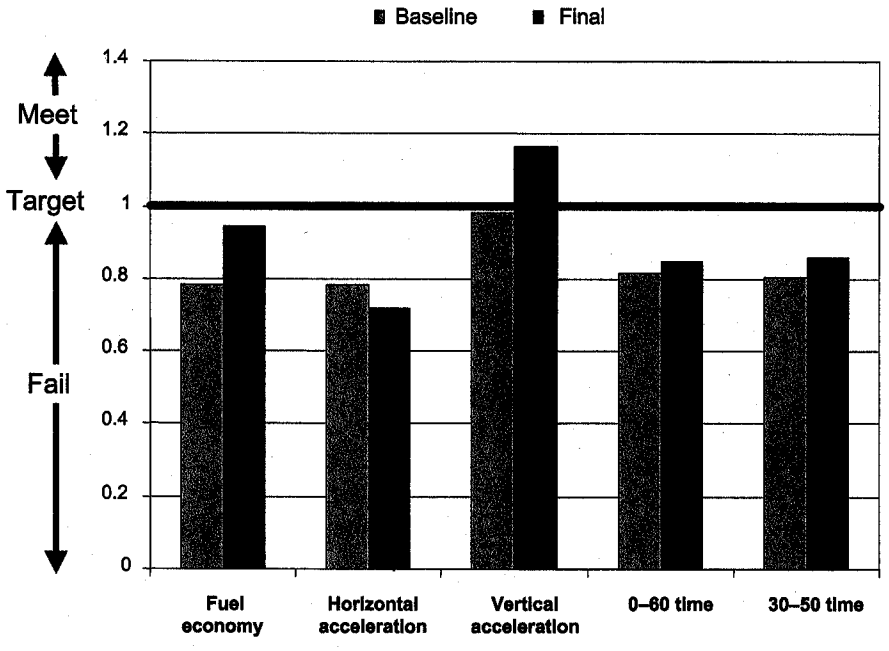

Figure 14 Achievement of set A targets.

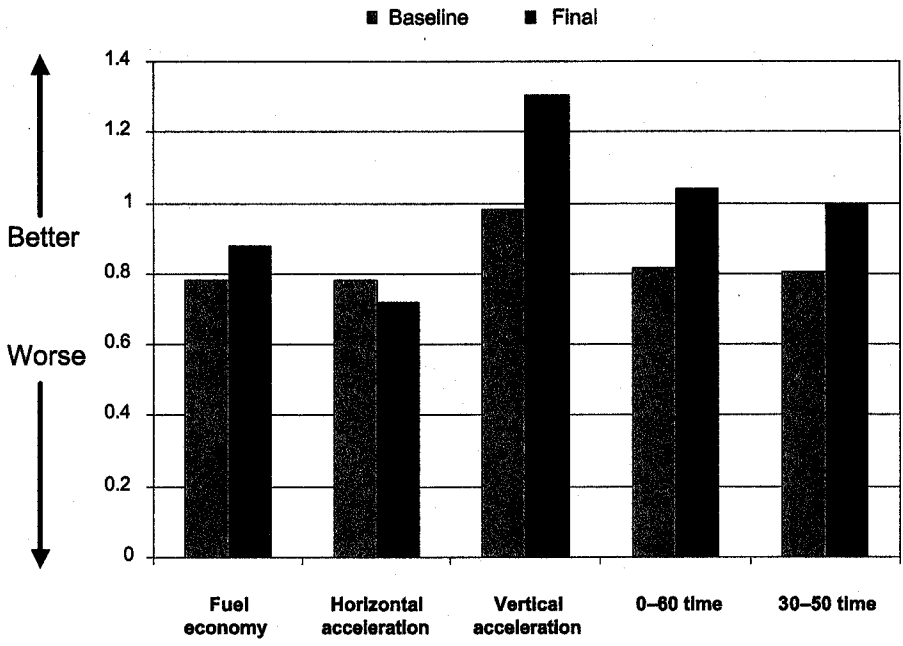

Figure 15 Achievement of set B targets.

target values such that achievement of targets corresponds to a value of one. For target set B, baseline and final values are normalized with respect to the target values of set A to enable a comparison between the results of the two sets. Compared to the results obtained for target set A, fuel economy decreases for target set B; however, it is still higher than that of the existing truck. On the other hand performance metrics are improved substantially, which indicates that another trade-off can be evaluated, namely that between fuel economy and performance. Driveability deteriorates even more, as expected. Ride quality improves moderately. The results obtained for the two different sets of targets indicate that target values as well as target weights play a significant role with respect to the outcome of the analytical target cascading process. One has to make decisions on the importance of different targets. For example, if fuel economy were more important than performance, the results for set A would be selected rather than those for set B, and vice-versa.

Baseline values are compared to final values of vehicle design variables and system responses for the vehicle-level problem in Table 3 for both sets of targets. Engine maps are compared and matched on a component basis during the optimization process. However, since maps are not scalar quantities but matrices, they are presented in terms of their Frobenius matrix norm. Superscripts $(\cdot)^{lb}$ and $(\cdot)^{ub}$ indicate variables at their lower or upper bounds, respectively. By inspecting the results of the vehicle-level problem (Table 3), it can be seen that the final values of many variables obtained for target set B are at their bounds, as opposed to those obtained for target set A. This can be explained by the fact that in the former case the optimizer is trying to achieve maximum improvement of the attributes that comprise the objective function, and therefore drives the design to the boundaries of the design space.

Table 3 Baseline and final values for vehicle design variables and system responses computed at the vehicle level for both target sets.

Variable	Type	Baseline value	Final value, target set A	Final value, target set B
Rear axle distance from CG [m]	Design	1.4235	1.2611	1.2000^{lb}
Mass moment of inertia [kgm^2]	Design	45194	40752	40109^{lb}
Front tyre compliance $\times 10^{-7}$ [m/N]	Design	5.95	5.37	4.5^{lb}
Rear tyre compliance $\times 10^{-7}$ [m/N]	Design	2.97	2.5^{lb}	2.5^{lb}
Front axle unsprung mass [kg]	Design	245	213	200^{lb}
Rear axle unsprung mass [kg]	Design	431	397	350^{lb}
Front suspension compliance $\times 10^{-6}$ [m/N]	Response	2.03	1.60^{lb}	1.60^{lb}
Front suspension damping [Ns/m]	Response	5000	5555	5996^{ub}
Rear suspension compliance $\times 10^{-7}$ [m/N]	Response	6.34	7.5^{ub}	6.26
Rear suspension damping [Ns/m]	Response	7000	7016	7996^{ub}
Engine map norm [Nm]	Response	11403	12261	11245
1st gear ratio [-]	Response	3.45	2.9068	3.0128
2nd gear ratio [-]	Response	2.24	1.8414	1.8914
3rd gear ratio [-]	Response	1.41	1.2502	1.2453
4th gear ratio [-]	Response	1.00	0.8129	0.8640

Table 4 Baseline and final values for engine design variables and responses computed at the system level for both target sets.

Variable	Type	Baseline value	Final value, target set A	Final value, target set B
Engine map norm [Nm]	Response	11403	12304	11257
Displacement [l]	Design	7.272	6.66	8.71
Compression ratio [-]	Design	18.0	18.1	15.79
Maximum boost pressure [atm]	Design	2.5	2.81	2.3
Wastegate activation point [rpm]	Design	1800	1710	2138
Inlet manifold pressure [atm]	Design	2.5	2.81	2.17
Injection timing [°]	Design	−10	−20	−15

Baseline values are compared to final values of engine design variables and responses for the system-level problem in Table 4 for both sets of targets. The baseline displacement and compression ratio specifications of the engine correspond to the International 7.3 l V8 engine type T444E. Inlet manifold pressure, boost characteristics, and injection timing vary according to operating conditions. Thus, initial values are chosen arbitrarily; final values represent optimal operating conditions for the respective configuration.

Initial values are compared to final values of design variables for the suspension and transmission system-level problems in Tables 5–7 for both sets of targets. Note that initial values are not baseline values for these problems. Thus, initial values of responses are meaningless and therefore not included.

Final values of system-level responses for both sets of targets are presented in Tables 4–7 to enable comparison with their respective values at the vehicle level shown in Table 3. Matching of responses within the analytical target cascading process is illustrated in Figure 16, based on the results obtained for target set A. Values are normalized with respect to the values obtained after solving the vehicle-level problem

Table 5 Initial and final values for transmission design variables and responses computed at the system level for both target sets.

Variable	Type	Initial value	Final value, target set A	Final value, target set B
1st gear ratio [-]	Response	—	2.9068	3.0116
2nd gear ratio [-]	Response	—	1.8436	1.8855
3rd gear ratio [-]	Response	—	1.2519	1.2444
4th gear ratio [-]	Response	—	0.8101	0.8067
Number of teeth, input ring [-]	Design	50	29	43
Number of teeth, input sun [-]	Design	30	16	24
Number of teeth, reaction ring [-]	Design	50	30	44
Number of teeth, reaction sun [-]	Design	30	14	22

Table 6 Initial and final values for front suspension design variables and responses computed at the system level for both target sets.

Variable	Type	Initial value	Final value, target set A	Final value, target set B
Compliance $\times 10^{-6}$ [m/N]	Response	—	1.5686	1.5990
Damping [Ns/m]	Response	—	5557.8	5999.9
Number of leaf springs [-]	Design	8	9	10^{ub}
Thickness [m]	Design	0.012	0.0104	0.0104
Radius [m]	Design	1.8	1.710	1.828
Width [m]	Design	0.15	0.0808	0.0721

Table 7 Initial and final values for rear suspension design variables and responses computed at the system level for both target sets.

Variable	Type	Initial value	Final value, target set A	Final value, target set B
Compliance $\times 10^{-7}$ [m/N]	Response	—	7.519	6.257
Damping [Ns/m]	Response	—	7016.2	7998.5
Number of leaf springs [-]	Design	8	6^{lb}	10^{ub}
Thickness [m]	Design	0.012	0.0176	0.014
Radius [m]	Design	1.8	2.244	4.225
Width [m]	Design	0.15	0.0524	0.0785

so that a percentage comparison for the deviation of the results obtained at the system level and the vehicle level (for the second iteration) is possible. The solutions obtained for the cascaded responses after solving the optimization problems at the vehicle and system levels iteratively are coordinated in order for the final design to be consistent. It can be seen that the mismatches are well below engineering tolerances, and therefore negligible: the process is assumed to be converged, and the final design is considered to be consistent.

It is emphasized that although design variables are obtained for all problems, design specifications for systems in this particular study (Table 3), and for systems, subsystems, and components in general, are the main outcome of the target cascading process.

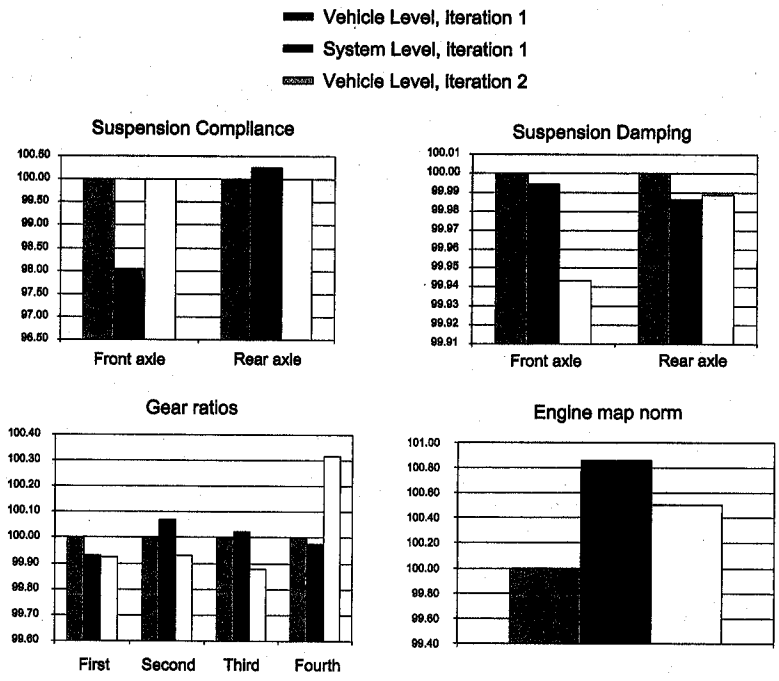

Figure 16 Matching of responses for target set A.

6 Conclusions

The target cascading process has been applied successfully for the redesign of an existing truck. The vehicle design problem was decomposed into a two-level hierarchy. After developing all necessary simulation and analysis models, powertrain and suspension design specifications of the truck for improved fuel economy, performance, and ride quality were determined with a minimum number of design iterations. Thus, vehicle design targets were translated into individual system design specifications. It was shown that systems can be outsourced and designed independently by means of (possibly different) optimization algorithms that are suitable for each problem. Moreover, the obtained final design of the vehicle is consistent through the coordination of the cascaded responses. Finally, trade-off relations between conflicting targets can be identified and evaluated. It can be concluded that the main benefit of the analytical target cascading process could be the reduction in vehicle design cycle time and the increased likelihood of physical prototype matching. In this manner, costly design iterations late in the development process can be avoided.

Acknowledgements

The authors would like to acknowledge the technical and financial support of the Automotive Research Center (ARC) by the National Automotive Center (NAC),

U.S. Army Tank Automotive and Armaments Command (TACOM), under contract DAAE07-98-R-L008. The ARC is a U.S. Army Centre of Excellence for Automotive Research at the University of Michigan, currently in partnership with the University of Alaska-Fairbanks, Clemson University, University of Iowa, Oakland University, University of Tennessee, Wayne State University, and University of Wisconsin-Madison. This research was partially supported by International Truck and Engine Corporation and Ford Motor Company. Finally, the authors would like to thank Umut Yildir for his help in developing the high fidelity suspension model.

References

1 20SIM (2001) *Pro User's Manual, Version 3.2*, The University of Twente – Controllab Products B.V., Enschede, The Netherlands.

2 Assanis, D., Delagrammatikas, G., Fellini, R., Filipi, Z., Liedtke, J., Michelena, N., Papalambros, P., Reyes, D., Rosenbaum, D., Sales, A. and Sasena, M. (1999) 'An Optimization Approach to Hybrid Electric Propulsion System Design', *Mechanics of Structures and Machines*, Vol. 27, No. 4, pp. 393–421.

3 Assanis, D.N., Filipi, Z.S., Gravante, S., Grohnke, D., Gui, X., Louca, L.S., Rideout, G.D., Stein, J.L. and Wang, Y. (2000) 'Validation and Use of Simulink Integrated, High Fidelity, Engine-in-Vehicle Simulation of the International Class VI Truck', In *Proceedings of the SAE World Congress*, Paper No. 2000-01–0288.

4 Assanis, D.N. and Heywood, J. (1986) 'Development and Use of a Computer Simulation of the Turbocompounded Diesel System for Engine Performance and Component Heat Transfer Studies', SAE Paper No. 86 0329.

5 Coleman, T., Branch, M.A., and Grace, A. (1999) *Optimization Toolbox for Use with MATLAB*, The MathWorks Inc., Natick, MA, version 2 Edn., January.

6 Delagrammatikas, G. and Assanis, D.N. (2001) 'The Reverse Engineering of a Turbocharged Diesel Engine Through a Unified Systems Approach', SAE Paper No. 2001-01–1244.

7 Demuth, H. and Beale, M. (2000) *Neural Network Toolbox for Use with MATLAB*. The MathWorks Inc., Natick, MA, version 4 Edn., September.

8 Heywood, J. (1988) *Internal Combustion Engine Fundamentals*, McGraw Hill, New York, NY.

9 Jones, D.R., Perttunen, C.D. and Stuckman, B.E. (1983) 'Lipschitzian Optimization without the Lipschitz Constant', *Journal of Optimization Theory and Applictations*, Vol. 79, pp. 157–181.

10 Karnopp, D.C., Margolis, D.L. and Rosenberg, R.C. (1990) *System Dynamics: A Unified Approach*, Wiley-Interscience, New York, NY.

11 Kim, H.M. (2001) *Target Cascading in Optimal System Design*, PhD thesis, University of Michigan, Ann Arbor, Michigan.

12 Kim, H.M., Michelena, N.F., Papalambros, P.Y. and Jiang, T. (2000) 'Target Cascading in Optimal System Design', In *Proceedings of the 26th Design Automation Conference*, Baltimore, MD, September. Paper No. 14265.

13 Lin, C.C., Filipi, Z., Wang, Y., Louca, L.S., Peng, H., Assanis, D. and Stein, J. (2001) 'Integrated, Feed-Forward Hybrid Electric Vehicle Simulation in Simulink and Its Use for Power Management Studies', SAE Paper No. 2001-01–1334.

14 Louca, L.S. (1998) *An Energy-Based Model Reduction Methodology for Automated Modeling*, PhD thesis, University of Michigan, Ann Arbor, Michigan.

15 Louca, L.S., Stein, J.L. and Hulbert, G.M. (1998) 'A Physical-Based Model Reduction Metric With an Application to Vehicle Dynamics'. In *Proceedings of the 4th IFAC Nonlinear Control Systems Design Symposium*, Enschede, The Netherlands.

16 Louca, L.S., Stein, J.L. and Rideout, D.G. (2001) 'Integrated Proper Vehicle Modeling and Simulation Using a Bond Graph Formulation', In *Proceedings of the International Conference on Bond Graph Modeling*, Phoenix, AZ, Published by the Society for Computer Simulation, San Diego, CA, ISBN 1-56555-221-0.

17 Michelena, N.F., Papalambros, P.Y., Park, H.A. and Kulkarni, D. (1999) 'Hierarchical Overlapping Coordination for Large-Scale Optimization by Decomposition', *AIAA Journal*, Vol. 37, pp. 890–896, July.

18 Millington, B.W. and Hartles, E.R. (1968) 'Frictional Losses in Diesel Engines', *SAE Transactions*, Vol. 77, Paper No. 68 0590.

19 Pacejka, H.B. and Bakker, E. (1993) 'Tyre Models for Vehicle Dynamics Analysis', In *Proceedings of the 1st International Colloquium on Tyre Models for Vehicle Dynamics Analysis*, Delft, The Netherlands.

20 Pacejka, H.B. and Tol, C.G.M. (1983) 'A Bond Graph Computer Model to Simulate the 3-Dimensional Dynamic Behaviour of a Heavy Truck', In *Proceedings of the Modeling and Simulation in Engineering, IMACS World Congress on Systems Simulation and Scientific Computation*, Montreal, Canada.

21 Rosenberg, R.C. and Karnopp, D.C. (1983) *Introduction to Physical System Dynamics*, McGraw-Hill, New York, NY.

22 SIMULINK. (2000) *Dynamic System Simulation for MATLAB, Version 4*, The MathWorks Inc., Natick, MA, November.

23 Tennekes, M. and Lumley, J.L. (1972) *A First Course in Turbulence*, MIT Press, Cambridge, MA.

24 Watson, N. and Janota, M.S. (1982) *Turbocharging the Internal Combustion Engine*, Wiley and Sons, New York, NY.

25 Watson, N., Pilley, A.D. and Marzouk, M. (1980) 'A Combustion Correlation for Diesel Engine Simulation', SAE Paper No. 80 0029.

Biographical notes

Hyung Min Kim is a Research Fellow in the Department of Mechanical Engineering at the University of Michigan. He received a BS and MS in Mechanical Engineering from the Korea Advanced Institute of Science and Technology (1995, 1997) and a PhD in Mechanical Engineering from the University of Michigan (2001). His interests include analytical target cascading, multidisciplinary optimization, product development methodology, and automotive design. Society memberships: ASME.

Michael Kokkolaras is a Research Fellow in the Department of Mechanical Engineering at the University of Michigan. He received a Diploma in Aerospace Engineering from the Munich University of Technology (1992) and a PhD in Mechanical Engineering from Rice University (1998). His interests include multidisciplinary analysis and design optimization, systems integration, and design of product families. Society memberships: ASME and AIAA.

Loucas S. Louca is an Assistant Research Scientist in the Department of Mechanical Engineering at the University of Michigan. He received a Diploma in Mechanical Engineering from the National Technical University of Athens (1992) and a MSE and PhD from the University of Michigan (1994, 1998). His interests

include physical model reduction, automated modelling, bond graphs, automatic control systems, and computer aided design. Society memberships: ASME and SCS.

George J. Delagrammatikas is a Research Fellow in the Department of Mechanical Engineering at the University of Michigan. He received a BS in Mechanical Engineering from the Massachusetts Institute of Technology (1995) and a MS and PhD in Mechanical Engineering from the University of Michigan (1996, 2001). His interests include automotive systems engineering, design optimization methodologies, multidisciplinary optimization, and renewable energy systems. Society memberships: ASME and SAE.

Nestor F. Michelena is an Associate Research Scientist in the Department of Mechanical Engineering at the University of Michigan. He received a BS and Eng from the Catholic University of Peru (1985, 1986), and a MS, MEng, and PhD from the University of California at Berkeley (1987, 1987, 1991). His interests include computational tools for large-scale systems design and optimization, systems and software integration, nonconventional vehicle systems, multicriteria optimization, and design of product families. Society memberships: ASME, INFORMS, ISSMO, AIAA, MPS, and SIAM.

Zoran S. Filipi is an Associate Research Scientist in the Department of Mechanical Engineering at the University of Michigan. He received a MS and PhD in Mechanical Engineering from the University of Belgrade (1987, 1992). His interests include modelling of engine physical processes and engine systems, turbocharging, heat transfer in DISI engines, HCCI engines and hybrid propulsion systems. Society memberships: SAE and ASME ICED Associate.

Panos Y. Papalambros is Donald C. Graham Professor of Engineering at the University of Michigan and Executive Director of the Automotive Research Center. He received a Diploma in Mechanical and Electrical Engineering from the National Technical University of Athens (1974) and a MS and PhD from Stanford University (1976, 1979). His interests include design methodology, optimization and systems integration, and ecologically conscious design. Society memberships: ASME Fellow, INFORMS, MPS, SIAM, SME, SAE, AIAA, ISSMO, and ASEE.

Jeffrey L. Stein is a Professor in the Department of Mechanical Engineering at the University of Michigan and Associate Director of the Automotive Research Center. He received a SB, SM, and PhD in Mechanical Engineering from the Massachusetts Institute of Technology, (1976, 1976, 1983). His interests include the use of proper dynamic mathematical models for engineering design, and the design, control, monitoring, and diagnosing of high performance machines with particular emphasis on machine tools and manufacturing systems. Society memberships: ASME, SME, and ASEE.

Dennis N. Assanis is Jon R. and Beverly S. Holt Professor of Engineering and Chair of the Department of Mechanical Engineering at the University of Michigan and Director of the Automotive Research Center. He received a BS in Marine Engineering from Newcastle University, England (1980), a SM in Naval Architecture and Mechanical Engineering, SM in Management of Technology, and PhD in Power and Propulsion from the Massachusetts Institute of Technology (1982, 1986, 1985). His interests include thermal sciences and their applications to automotive systems design, and computer simulation and validation of internal combustion engine processes and systems. Society memberships: ASEE, ASME ICED Associate, SNAME, Combustion Institute, and SAE Fellow.